UCLA
UCLA Previously Published Works

Title

Desynchronization and Plasticity of Striato-frontal Connectivity in Major Depressive Disorder.

Permalink

https://escholarship.org/uc/item/7ks2991n

Journal

Cerebral Cortex, 26(11)

ISSN

1047-3211

Authors

Leaver, Amber M
Espinoza, Randall
Joshi, Shantanu H
et al.

Publication Date

2016-10-01

DOI

10.1093/cercor/bhv207

Peer reviewed

OXFORD

ORIGINAL ARTICLE

Desynchronization and Plasticity of Striato-frontal Connectivity in Major Depressive Disorder

Amber M. Leaver[1], Randall Espinoza[2], Shantanu H. Joshi[1], Megha Vasavada[1], Stephanie Njau[1], Roger P. Woods[1,2] and Katherine L. Narr[1,2]

[1]Ahmanson-Lovelace Brain Mapping Center, Department of Neurology, and [2]Department of Psychiatry and Biobehavioral Sciences, University of California Los Angeles, Los Angeles, CA 90095, USA

Address correspondence to Katherine L. Narr, 635 Charles E Young Dr S #225, University of California Los Angeles, Los Angeles, CA 90095, USA.
Email: narr@ucla.edu

Abstract

Major depressive disorder (MDD) is associated with dysfunctional corticolimbic networks, making functional connectivity studies integral for understanding the mechanisms underlying MDD pathophysiology and treatment. Resting-state functional connectivity (RSFC) studies analyze patterns of temporally coherent intrinsic brain activity in "resting-state networks" (RSNs). The default-mode network (DMN) has been of particular interest to depression research; however, a single RSN is unlikely to capture MDD pathophysiology in its entirety, and the DMN itself can be characterized by multiple RSNs. This, coupled with conflicting previous results, underscores the need for further research. Here, we measured RSFC in MDD by targeting RSNs overlapping with corticolimbic regions and further determined whether altered patterns of RSFC were restored with electroconvulsive therapy (ECT). MDD patients exhibited hyperconnectivity between ventral striatum (VS) and the ventral default-mode network (vDMN), while simultaneously demonstrating hypoconnectivity with the anterior DMN (aDMN). ECT influenced this pattern: VS-vDMN hyperconnectivity was significantly reduced while VS-aDMN hypoconnectivity only modestly improved. RSFC between the salience RSN and dorsomedial prefrontal cortex was also reduced in MDD, but was not affected by ECT. Taken together, our results support a model of ventral/dorsal imbalance in MDD and further suggest that the VS is a key structure contributing to this desynchronization.

Key words: connectivity, default-mode network, depression, limbic, ventral striatum

Introduction

Current models describe major depressive disorder (MDD) as a brain-network disorder affecting fronto-limbic and fronto-striato-thalamic circuits (Mayberg 1997; Gotlib and Joormann 2010; Price and Drevets 2012). Neurostimulation treatments attempt to correct aberrant neural transmission in these networks by delivering electric or magnetic stimulation to implicated brain regions. Some therapies target structures directly, including subgenual anterior cingulate (deep brain stimulation, DBS), ventral striatum (DBS), and dorsolateral prefrontal cortex (transcranial magnetic and direct-current stimulation, TMS and tDCS, respectively; [Hauptman et al. 2008; De Raedt et al. 2014]). Electroconvulsive therapy (ECT) is less focal and yet most effective at reducing symptoms of depression, eliciting generalized seizures associated with more widespread neural changes (Perrin et al. 2012; Abbott et al. 2013; Tendolkar et al. 2013; Zhang et al. 2013; Dukart et al. 2014; Lyden et al. 2014; van Waarde et al. 2015; Joshi et al. 2015). However, the exact nature of network dysfunction responsible for depressive disorders, and how this dysfunction is best targeted by current neurostimulation therapies, remains poorly understood.

Connectivity analyses of human neuroimaging data will be critical for achieving a network-level understanding of MDD neuropathophysiology. A popular approach is to use resting-state functional connectivity (RSFC) to identify and analyze networks

that share temporally coherent patterns of intrinsic brain activity or "resting-state networks" (RSNs). The default-mode network (DMN) has been of particular interest to depression research, given the role this network is thought to play in self-referential processing (Raichle et al. 2001; Morcom and Fletcher 2007; Spreng and Grady 2010) and its overlap with structures previously implicated in MDD like the hippocampus (Sheline et al. 1999) and medial cortical regions (Drevets et al. 1997; Mayberg et al. 1999). Studies of MDD have identified hyperconnectivity between the DMN and specific brain regions including ventral anterior cingulate and adjacent ventromedial prefrontal cortex (Greicius et al. 2007; Manoliu et al. 2013), mediodorsal thalamus (Greicius et al. 2007), and dorsolateral prefrontal cortex (Sheline et al. 2009). More recently, connectivity between the DMN and other RSNs has been considered, particularly with RSNs involving lateral prefrontal regions (e.g., "task-positive" networks [Hamilton, Furman, et al. 2011; Manoliu et al. 2013]).

Studying RSNs allows examination of well-characterized large-scale networks that have been studied in other contexts and disorders; however, there are potential confounding factors. RSNs may be defined in different ways across studies. The DMN, for example, can be identified using seed regions defined a priori or data-driven independent component analysis (ICA). Furthermore, the DMN can be identified either as a single network or as many related networks (Fox et al. 2005; Uddin et al. 2009). Finally, it is unlikely that any single RSN captures the heterogeneous clinical presentation of MDD; rather, RSNs are perhaps best used as a tool to probe the function of brain regions hypothesized as most relevant to MDD pathophysiology. When also considering the challenge of recruiting adequately large and homogenous cohorts to study MDD and other disorders, or to study specific clinical or neuropsychological deficits that may better link with the underlying neuropathophysiology across disorders (Insel et al. 2010), it is clear that validation of past results with new approaches is crucial.

In the current study, we assessed differences in patterns of intrinsic, spontaneous activity between MDD patients and demographically matched healthy volunteers using ICA of resting-state functional magnetic resonance imaging (MRI). We aimed to measure changes associated both with the diagnosis of MDD and with treatment response measured by examining patients before and after they received an index treatment series of ECT. We specifically targeted limbic and medial cortical structures by measuring 6 previously characterized RSNs (Damoiseaux et al. 2006; Smith et al. 2009; Allen et al. 2011; Laird et al. 2011), including 3 DMNs, the Salience Network (Sal-N), an orbitofrontal network (OFN), and an RSN covering the thalamus and ventral basal ganglia (Th/BG-N; Fig. 1). In this way, we hoped to elucidate the striato-thalamo-frontal and limbic circuits impaired in MDD.

Materials and Methods

Participants

Thirty-three patients (13 males, age mean/SD = 43.55/13.78 years) and 33 demographically similar healthy volunteers (14 males, age mean/SD = 39.33/12.48 years) gave informed written consent to participate in this UCLA IRB-approved study. All patients were diagnosed with MDD (unipolar; DSM-IV-TR) and had failed to respond to at least 2 prior antidepressant therapies (i.e., were classified as "treatment resistant"). Patients with comorbid psychiatric or neurological disorders or concurrent serious illness were excluded. All patients ceased benzodiazepine, antidepressant, and/or anti-anxiety drugs at least 48–72 h prior to

the study and had not received neuromodulation treatment within 6 months prior to the study (i.e., ECT, transcranial magnetic stimulation, or vagal nerve stimulation). For healthy volunteers, exclusion criteria were as follows: any history of serious illness, neurological disorders, or psychiatric disorders [assessed using the Mini-International Neuropsychiatric Interview, MINI (Sheehan et al. 1998)]. Depressive symptoms were assessed in patients using the Hamilton Depression Inventory (HAMD, 17-item); patients with HAMD scores <21 were not included in this study. Additional measures (Montgomery Åsberg Depression Rating Scale and Quick Inventory of Depressive Symptomatology) were strongly intercorrelated with HAMD scores; thus, we report only HAMD measures in this manuscript. Participant characteristics are given in Table 1.

Study Visits and ECT

Patients completed 3 MRI scans: 1) within 24 h before first ECT session (baseline), 2) immediately before their third ECT appointment, and 3) after their ECT index series as clinically determined (2–4 weeks after baseline). Twenty-four patients returned for the third timepoint; only these patients were used in analyses assessing treatment response, and they received either right unilateral ECT (RUL; $n = 18$) or a combination of right unilateral and bifrontal ECT (RUL + BF; $n = 6$) using standard procedures (d'Elia 1970; Zhang et al. 2013; Lyden et al. 2014), 3 times a week during the index series (mean/SD number of treatments = 11.79/3.34; Table 1) at UCLA Resnick Neuropsychiatric Hospital. A group of healthy never-depressed "control" volunteers were also scanned twice, at baseline and at a 2- to 4-week follow-up, to establish normative values and test–retest reliability of resting-state fMRI variables.

Image Acquisition and Preprocessing

Using a 3T Siemens Allegra scanner, 180 functional images were acquired: TR = 2.0 s, TE = 30 ms, flip angle = 70°, 34 axial slices, 3.4 × 3.4 × 5 mm³ resolution. A high-resolution T_1-weighted anatomical scan (MPRAGE) was also collected at each session. Functional images were preprocessed using standard protocols in FSL v 5.0 (FMRIB, Functional MRI of the Brain), including slice-time correction, rigid-body motion correction (6 degrees of freedom, aligned to middle volume), high-pass filter (0.01 Hz), and spatial smoothing (6 × 6 × 6 mm³). Two leading functional volumes were discarded prior to preprocessing. Additionally, spin-history artifacts resulting from interleaved slice acquisition (often correlated with head motion [Friston et al. 1996]) were removed from voxel time courses using ICA and FSL's *regfilt*. Briefly, ICA was run separately on each subject's fMRI data, and ICs representing spin-echo artifacts were identified by 1 deciding observer and confirmed by a second observer (average interrater agreement was 85%). Artifact ICs were then removed from voxel time courses by taking the residuals from a linear regression using noisy IC time courses as regressors. Preprocessed and denoised images were aligned to each subject's MPRAGE first within each session and then aligned across sessions to the MPRAGE from the first scan using FSL. Finally, images were normalized to MNI standard space using a nonlinear transformation and interpolated to 2 × 2 × 2 mm³ resolution in SPM8 (Wellcome Trust Centre for Neuroimaging).

Mean relative displacement (MRD) values were calculated during motion-correction procedures in FSL as described above and were analyzed to confirm that head motion did not differ on average between scans (Satterthwaite et al. 2013). MRD was
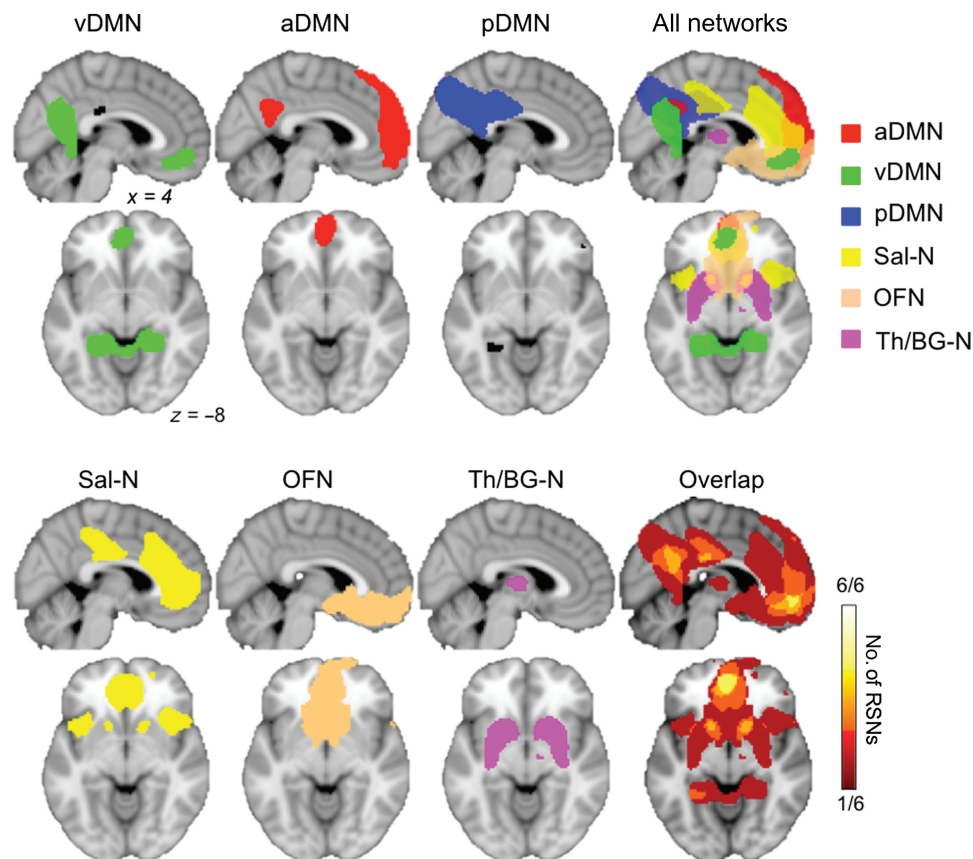
Figure 1. Corticolimbic RSNs examined for MDD-related effects. Maps of the 6 networks of interest are displayed on averaged template brains in the left 3 columns; color indicates which RSN is displayed (key at upper right, all $P < 0.00001$). For all maps, black marks voxels negatively correlated with the RSN. In the upper right panel, all networks are superimposed on the same brain. In the bottom right panel, a map displaying the degree of spatial overlap between RSNs is shown, where color indicates the number of RSNs represented in each voxel (key at bottom right). Note that overlap is determined by map thresholds determined a priori. Networks include ventral, anterior, and posterior default-mode networks (vDMN, aDMN, pDMN, respectively), salience network (Sal-N), orbitofrontal network OFN, and thalamus/basal ganglia network (Th/BG-N).

Table 1 Participant characteristics

	Sex	Age	Age at 1st MDD episode	ECT placement	Total no. of ECT sessions	HAMD scores		
						1	2	3
MDD ($n = 33$)	13 m,20 f	43.5 (13.8)	26.0 (13.9)	24 RUL, 9 Other[a]	11.8 (3.3)	26.5 (4.8)	21.0 (5.3)	12.1 (7.7)
Healthy ($n = 33$)	14 m,19 f	39.3 (12.5)	n/a	n/a	n/a	n/a	n/a	n/a
t-test[b] (P value)	0.06 (0.80)	1.3 (0.20)	n/a	n/a	n/a	n/a	5.4 (0.7×10^{-6})	7.9 (0.6×10^{-6})

Note: HAMD, Hamilton Depression Rating Scale; RUL, right unilateral; n/a, not applicable.
[a]Patients not receiving RUL ECT had a combination of RUL and bifrontal (BF) treatment.
[b]Chi-squared test was applied to sex, unpaired t-test compared age between groups, and paired t-tests compared changes in HAMD score from baseline with ECT.

not different in patients and healthy volunteers during baseline scans (mean/SD = 0.11/0.06 mm for both; $t_{64} = -0.18$, $P = 0.86$). Additionally, MRD did not change between baseline and follow-up scans for patients ($t_{23} = -0.99$, $P = 0.33$) or healthy participants ($t_{30} = -0.13$, $P = 0.90$). Note that single-subject denoising to remove spin-echo artifacts (which are often caused by head motion) is also likely to ameliorate potential effects of head motion in subsequent statistical analyses, in addition to standard motion-correction procedures in FSL.

Defining RSNs

To identify RSNs, ICA was run using established procedures in FSL MELODIC. All functional images were concatenated, and the optimal number of independent components was estimated with probabilistic ICA (Beckmann and Smith 2004); 29 group ICs were identified with this approach, each comprised a spatial map and time course. Upon visual inspection, spatial maps from 24 ICs overlapped gray matter and were identified as RSNs, and the remaining overlapped white matter and/or cerebrospinal fluid and were thus considered unlikely to correspond with neural function. Six RSNs were targeted as networks of interest (Fig. 1), which covered medial corticolimbic areas previously implicated in depression and emotional processing. These 6 RSNs were selected and verified visually by study coauthors, and have been reliably demonstrated in healthy volunteers in previous research (Damoiseaux et al. 2006; Smith et al. 2009; Allen et al. 2011; Laird et al. 2011). To reduce the number of

Table 2 MNI coordinates

Analysis	RSN	Region	MNI coordinates			Volume (mm^3)
			X	Y	Z	
RSNs	Ventral default-mode network	Posterior cingulate cortex	−8	−54	8	n/a
	Anterior default-mode network	Medial prefrontal cortex	0	52	8	n/a
	Posterior default-mode network	Precuneus	−4	−70	36	n/a
	Salience network	Dorsal anterior cingulate cortex	0	32	22	n/a
	Orbitofrontal network	Left medial orbitofrontal cortex	−10	26	−18	n/a
	Thalamus/basal ganglia network	Right ventral striatum	26	2	−12	n/a
MDD vs. HC	Ventral default-mode network	Ventral striatum	15.1	15.3	−13	144
	Anterior default-mode network	Ventral striatum	14.8	11.8	−10.6	112
	Salience network	Dorsomedial prefrontal cortex	5.69	56	11.8	160

Note: Peak coordinates are reported for RSNs, and center-of-gravity coordinates are reported for between-groups analyses (MDD vs. HC).
RSN, resting-state network; MDD, major depressive disorder; HC, healthy controls.

second-level statistical tests performed, analyses were restricted to voxels surviving a strict threshold ($P < 0.00001$) in any of the 6 RSN group maps (Fig. 1). Peak voxels for each RSN are reported in Table 2 to facilitate comparisons with past and future studies using seed regions to define RSNs.

Prior to second-level statistical analysis, single-subject RSNs were derived using dual regression per standard procedures in FSL. Though described in more detail elsewhere (Filippini et al. 2009), we briefly describe this standard procedure here. Each subject's data were submitted to a multiple regression analysis, where all spatial maps from the group probabilistic ICA (described above) were used as regressors. This yielded a unique set of timeseries for each subject, one for each group spatial map. These timeseries were then used as regressors in a second multiple regression analysis to derive spatial maps of all components. Second-level statistics (described in the following section) were performed on subject-specific spatial maps corresponding to our 6 RSNs of interest. Thus, in each RSN map for each subject, the value (z-score) of a given voxel corresponded to the relative temporal coherence (or "functional connectivity") of that voxel with the corresponding RSN. Global signal was not removed in these analyses (for discussion of both sides of this controversial issue, refer to Fox et al. (2009); Murphy et al. (2009)).

Second-Level Statistical Analyses

To determine differences in functional connectivity between patients and healthy participants, we used voxelwise t-tests to compare RSFC values (z-scores) between groups within each RSN, using a single-voxel (i.e., height) threshold of $P < 0.0005$ and cluster threshold of $k > 10$ voxels. This cluster threshold was chosen so as not to bias findings against subcortical nuclei, in which the spatial extent of statistical effects (i.e., cluster size) is limited by the size of the structure/nucleus. In clusters resulting from these between-groups t-tests, region of interest (ROI) analyses were performed in patients to measure correlations (Pearson's r) between RSN RSFC values and 2 variables: HAMD scores and duration of illness (in years).

To measure treatment response, we performed ROI analyses restricted to patients who completed the third MRI scan (after ~2–4 weeks of ECT, n = 24) and with Bonferroni correction for the number of tests in each ROI. First, we used t-tests to compare RSN RSFC z-scores between all timepoints. Pairwise t-tests were chosen to accommodate different numbers of timepoints between groups (3 timepoints for patients, 2 timepoints for healthy volunteers) and to accommodate non-monotonic changes across

timepoints in patients (e.g., RSFC z-scores may increase from baseline to the second visit, but then decrease on the third visit). Then, we measured correlations (Pearson's r) between changes in RSFC and changes in depressive symptoms (HAMD scores). Finally, we confirmed that ECT-related changes in RSFC were not affected by head motion or lead placement by using these factors (MRD; RUL vs. RUL + BF) as nuisance covariates in a post hoc analysis of covariance. As these post hoc tests were performed to confirm that these factors did not contribute to our results, multiple comparison correction was not applied.

Results

Corticolimbic RSNs

Three DMNs were identified: 1) a ventral DMN (vDMN) including ventromedial prefrontal cortex (PFC), posterior cingulate cortex (PCC) and adjacent precuneus, and bilateral hippocampus, 2) an anterior DMN (aDMN) including medial PFC and PCC, and 3) a posterior DMN (pDMN) including PCC and adjacent precuneus. Additional networks chosen were: 4) the Salience Network (Sal-N) including the anterior cingulate cortex (ACC) and adjacent medial PFC, mid-cingulate cortex, bilateral insula, dorsolateral PFC, and bilateral ventral striatum (VS), 5) an OFN including orbitofrontal cortex, VS, and basal forebrain, and 6) an RSN including the basal ganglia and thalamus (Th/BG-N). All 6 RSNs have been reliably demonstrated in healthy volunteers in previous research (Damoiseaux et al. 2006; Smith et al. 2009; Allen et al. 2011; Laird et al. 2011). Regions of overlap across >50% of networks included ventromedial PFC (4/6 RSNs), PCC/precuneus (4/6 RSNs), dorsal PCC (3/6 RSNs), and VS (3/6 RSNs); points of overlap are reported for reference and determined by thresholds chosen a priori ($P < 0.00001$). Maps are displayed in Figure 1, and peak coordinates are given in Table 2.

Altered Functional Connectivity in MDD

Depressed patients exhibited aberrant RSFC with respect to 3 RSNs (Table 2). In MDD patients, intrinsic activity the right ventral striatum (VS) was negatively correlated (or "anti-correlated") with the ventral DMN (Fig. 2A). In comparison, healthy participants had significantly less connectivity between VS and vDMN. In contrast, in healthy volunteers, right VS activity was negatively correlated with the aDMN, and MDD patients showed significantly less VS-to-aDMN connectivity (Fig. 2B). Taken together, these results demonstrate that MDD patients exhibit hyperconnectivity between VS and vDMN, while simultaneously exhibiting
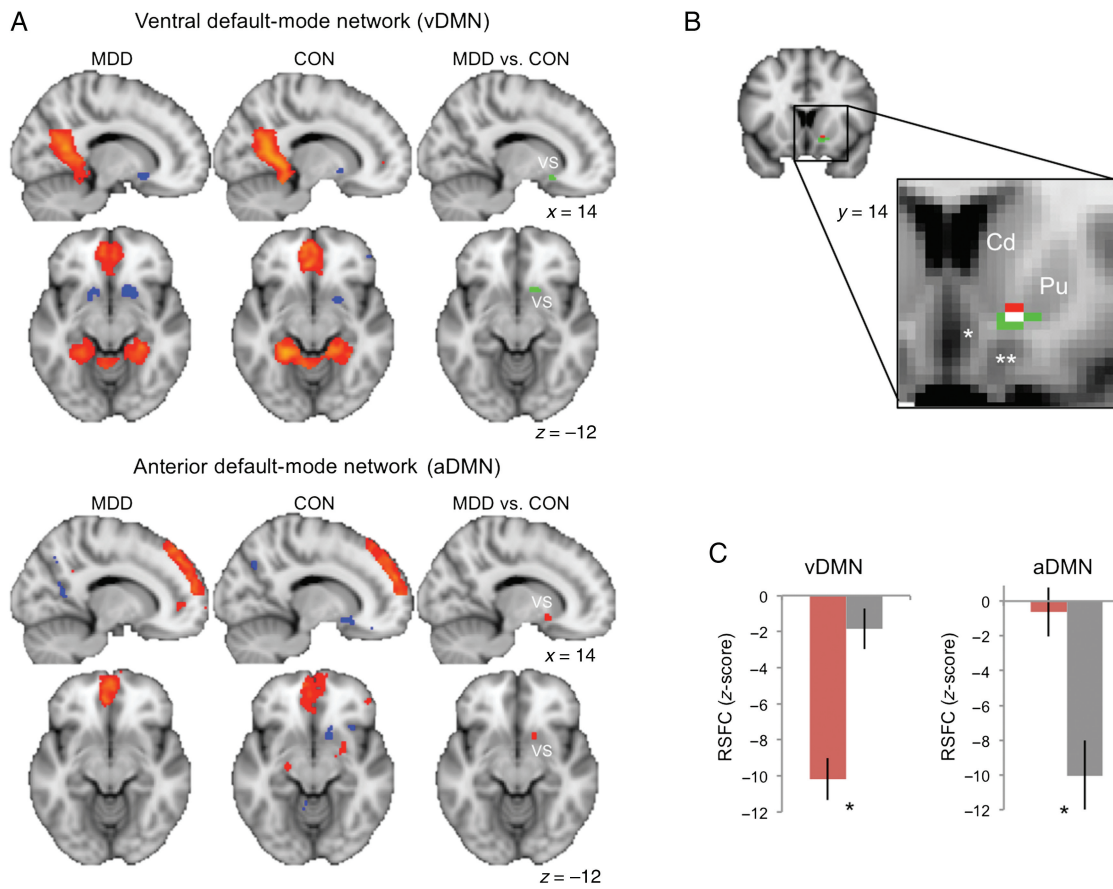
Figure 2. Ventral striatum (VS) RSFC is altered in MDD. (A) The results of 1-sample t-tests for MDD patients (left) and controls (middle) are displayed for the vDMN (top rows) and aDMN (bottom rows). Orange marks voxels exhibiting positive temporal coherence with each network, and blue marks instances of negative temporal coherence ($P < 0.00001$). At right, results of 2-sample t-tests comparing RSFC between MDD patients and healthy controls are displayed in green for vDMN and red for aDMN ($P < 0.0005$, $k > 10$). (B) Both between-groups effects shown in A are displayed on the same coronal section, with overlapping voxels marked in white. Slice is enlarged in the inset to show surrounding anatomy, including the caudate (Cd), putamen (Pu), subgenual anterior cingulate (single asterisk), and gyrus rectus of the orbitofrontal cortex (double asterisk). (C) Bar charts display mean RSFC between VS and DMNs for patients (red) and controls (grey); asterisk denotes significance determined by voxelwise tests. In all images and figures, statistical maps are displayed on MNI template brains in neurological convention.

hypoconnectivity with the aDMN. In the Salience network, functional connectivity was reduced with the dorsomedial prefrontal cortex (dmPFC) in MDD patients compared with healthy participants (Fig. 3). In ROI analyses, functional connectivity in these regions (with respect to corresponding RSNs) was not correlated with depressive symptoms (HAMD scores), duration of illness, or mean head motion during the scan ($P > 0.05$).

Treatment Response in Regions of Aberrant RSFC

Symptoms of depression were significantly reduced after ECT ($P < 0.00001$; Table 1), with 14 of 24 returning patients experiencing ≥50% reduction in HAMD score, and 6 patients meeting a strict criterion for remission (HAMD score ≤7 [Zimmerman et al. 2012]). ROI analyses were performed to determine whether treatment with ECT restored RSFC in regions identified to have altered RSFC in MDD patients at baseline (Fig. 4). In VS, hyperconnectivity with the vDMN was reduced with treatment, including after 2 ECT sessions ($P_{corr} < 0.05$) and after 2–4 weeks of ECT (at completion of the ECT treatment index series) ($P_{corr} < 0.05$). Treatment also reduced hypoconnectivity between VS and aDMN; however, this effect was less pronounced. Hypoconnectivity was significantly reduced after 2 ECT sessions ($P_{corr} < 0.05$) and only moderately reduced after 2–4 weeks of ECT (uncorrected $P = 0.03$). ECT did not

significantly affect RSFC between dmPFC and Sal-N, though weak trends toward restored RSFC were found (after 2 ECT uncorrected $P = 0.02$; after 2–4 weeks uncorrected $P = 0.11$). In all ROIs, RSFC did not differ between baseline and follow-up scans in healthy volunteers ($P > 0.05$).

In post hoc analyses, no correlations between changes in RSFC and changes in HAMD scores were significant ($P > 0.05$). Additionally, changes in RSFC (baseline vs. 2–4 week follow-up) were analyzed a second time while using head motion and ECT lead placement as nuisance covariates. Effects reported in the main analyses remained: significant changes in VS-vDMN connectivity persisted ($P < 0.01$ for both), while trends were present for changes in VS-aDMN connectivity ($P = 0.06$ when controlling for lead placement; $P = 0.08$ when controlling for head motion). Again, RSFC between dmPFC and Sal-N was not strongly affected by ECT ($P = 0.31$ when controlling for lead placement; $P = 0.16$ when controlling for head motion). No significant interactions were present in these analyses.

Discussion

Here, we report aberrant patterns of functional connectivity in patients with MDD. First, we demonstrated that, in MDD, the ventral striatum exhibits different functional relationships with the
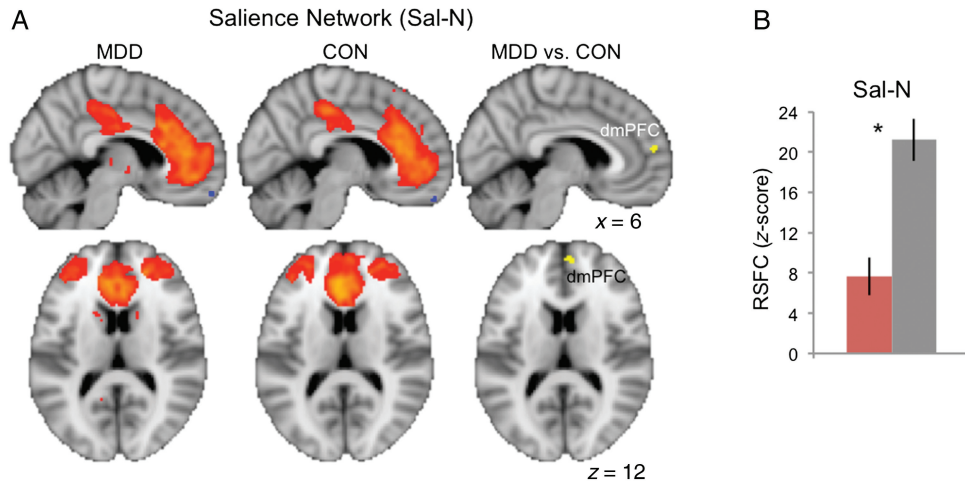
Figure 3. Decreased RSFC in dmPFC with MDD. (A) One-sample *t*-tests for MDD patients (left) and controls (middle images) display the Salience Network (Sal-N, *P* < 0.00001). At right, results of a 2-sample *t*-test comparing RSFC between MDD patients and healthy controls are displayed in yellow for the Sal-N (*P* < 0.0005, *k* > 10). (B) Bar chart displays mean FC between dmPFC and Sal-N for patients (red) and controls (grey); asterisk denotes significance determined by voxelwise test.
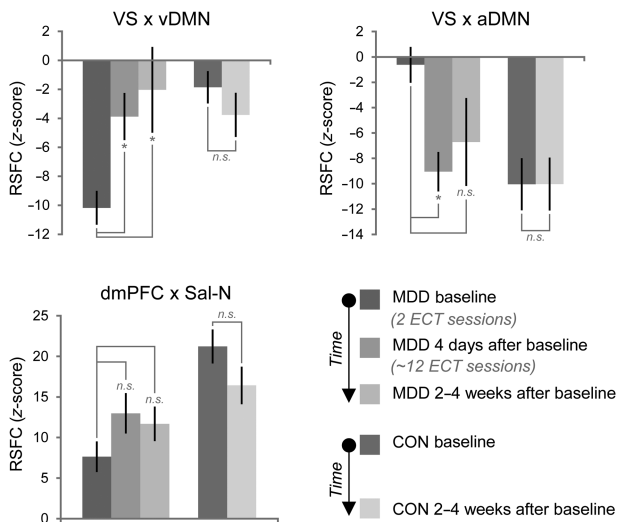

Figure 4. Aberrant RSFC in ventral striatum is restored by ECT. For regions identified to have altered RSFC in MDD patients, bar charts plot the mean RSFC *z*-score for each timepoint and group (key given at lower right). The results of pairwise *t*-tests between baseline and follow-up scans within each group are marked, where asterisks indicate $P_{corr} < 0.05$ and "n.s." marks pairs that were not significantly different ($P_{corr} > 0.05$).

ventral and anterior DMNs, which involve structures thought to be hyper- and hyporesponsive in MDD, respectively (Mayberg 1997; Koenigs and Grafman 2009; Price and Drevets 2012). Furthermore, we demonstrate that this abnormal pattern of RSFC is normalized with a highly effective neurostimulation therapy, ECT, particularly with regard to functional relationships between VS and ventral DMN. Additionally, we report reduced connectivity between dorsomedial PFC and the Salience RSN, which contains the ACC, anterior insula, and VS. This effect mirrors hypoconnectivity between VS and anterior DMN, which overlaps dorsomedial PFC. As a whole, our data lend further support to the hypothesis that depression involves an imbalance between hyporesponsive dorsal and hyperresponsive ventral structures (Mayberg 1997; Drevets 2000; Koenigs and Grafman 2009) and place new

emphasis on a key structure involved in that imbalance, the ventral striatum.

Ventral Striatum as a Critical Component of Network-Level Dysfunction in MDD

At rest, spontaneous fMRI activity in any given voxel (e.g., in the VS) is a mixed signal reflecting the functional connections of its thousands of neurons with various different brain circuits. Like a microphone at a cocktail party, a single voxel's time course is a "recording" of this mixture of signals, or functional connections. In our study, we used ICA to examine RSFC in 6 RSNs that, although statistically dissociated, were not entirely spatially dissociable. In this way, we simultaneously examined the different functional connections of regions that overlapped across RSNs at specific thresholds, like the VS and medial PFC (Fig. 1). This is a critical departure from previous studies, which examined only dominant patterns of connectivity using 1) seed region analysis (Bluhm et al. 2009; Sheline et al. 2009; Hamilton, Chen, et al. 2011; Hamilton, Furman, et al. 2011) or 2) single RSNs defined using ICA (Greicius et al. 2007). For example, although previous seed-region studies in healthy individuals have demonstrated that the primary pattern of RSFC in the VS involves the orbitofrontal cortex (Di Martino et al. 2008), our approach statistically removed this dominant signal (i.e., the OFN, Fig. 1) allowing examination of other connectivity patterns of the VS. The same restriction applies to previous studies using ICA to identify a limited number of networks (Greicius et al. 2007), where medial PFC regions are not dissociated across RSNs. Thus, our approach may offer a complementary, and perhaps more comprehensive, analysis of the complex networks that differentially recruit medial PFC and VS, rather than the dominant signal (or loudest voice at the cocktail party).

The VS, like other basal ganglia substructures, is involved in striato-thalamo-cortical loops implicated in motivation, reward, and assessing positive and negative value of stimuli (Cardinal et al. 2002; Kable and Glimcher 2009; Price and Drevets 2012). These circuits involve reciprocal prefrontal connections, including both direct projections from medial PFC to VS (Ferry et al. 2000; Ongür and Price 2000) and indirect projections from VS to medial PFC via the ventral pallidum and mediodorsal thalamus (Ray and Price 1993; Ongür and Price 2000). In the current study, VS

exhibited opposing patterns of MDD-related RSFC effects with different medial prefrontal networks. Specifically, VS exhibited greater (negative) temporal coherence with ventral DMN and less (negative) temporal coherence with anterior/dorsal DMN. Although these opposing effects overlapped spatially within the VS, they likely reflect separate effects in different circuits: differential modulation of different VS neurons by separate medial PFC regions (or vice versa). Indeed, VS neurons connect with regions throughout the ventral and dorsal medial PFC in animal studies using tracer injections (Ray and Price 1993; Ferry et al. 2000; Ongür and Price 2000). Representations of positively and negatively valenced stimuli are also spatially dissociable within the VS in humans (Seymour et al. 2007) and other animals (Reynolds and Berridge 2002), suggesting that both function and network connections are separable in this region. Thus, the VS (and by extension the ventral pallidum and mediodorsal thalamus) is likely involved in separable dysfunctional circuits in MDD. Furthermore, these striato-thalamo-frontal circuits may also be differentially influenced by other inputs to the VS (e.g., ventral tegmental area, amygdala, hippocampus [Mayberg 1997; Price and Drevets 2012]). Future animal work, or simultaneous DBS-neuroimaging studies, targeting these circuits more precisely may be better able to functionally parse these and other networks in the context of MDD.

Ventral/Dorsal Imbalance in MDD

Our results support that multiple, separable striato-thalamo-cortical circuits may be dysfunctional in MDD, as hypothesized previously (Mayberg 1997; Price and Drevets 2012). These findings lead us to further posit that these network effects relate to the proposed imbalance between hyperresponsive ventral regions and hyporesponsive dorsal regions in MDD (Ressler and Mayberg 2007; Koenigs and Grafman 2009; Price and Drevets 2012). Previous studies show that ventral limbic structures are hyperresponsive in depression, including the subgenual ACC and adjacent ventromedial PFC (Greicius et al. 2007), amygdala (Sheline et al. 2001; Victor et al. 2010), and VS (Greicius et al. 2007; Furman et al. 2011). Accordingly, we reported increased temporal coherence, or hyperconnectivity, in MDD between VS and ventral DMN, which included ventromedial PFC, ventral PCC/precuneus, and the hippocampus. Previous studies have also reported hyporesponsiveness in dorsal brain regions with depression, including dorsolateral and dorsomedial PFC (Galynker et al. 1998; Siegle et al. 2007) and reduced connectivity between striatum and dorsal ACC in both unipolar and bipolar depression (Anand et al. 2005, 2009). Compatible with these results, we also show reduced RSFC between anterior DMN (including anterior and dorsomedial PFC) and VS, and between the dorsomedial PFC and the Salience Network (including ACC, dorsomedial PFC, anterior insula, VS, and dorsolateral PFC).

Though the precise symptoms emanating from this ventral/dorsal imbalance remain unclear, the dorsomedial PFC, perhaps with lateral PFC, may be responsible for successful emotion regulation, while ventral/limbic regions generate the experience of negative affect and mood (Ressler and Mayberg 2007; Koenigs and Grafman 2009; Gotlib and Joormann 2010; Price and Drevets 2012). However, positive affect is also supported by ventral limbic structures like VS, ventromedial PFC, and amygdala (Reynolds and Berridge 2002; Murray 2007; Seymour et al. 2007; Winecoff et al. 2013). MDD patients have exhibited reduced responses to positive and/or rewarding stimuli in VS (Epstein et al. 2006; Pizzagalli et al. 2009; Robinson et al. 2012) and other ventral limbic regions (Groenewold et al. 2013), so perhaps dysfunction and/or dysregulation of ventral structures results in both increased negative affect/mood and decreased positive affect/mood, though such relationships require empirical confirmation. In MDD, impaired emotion regulation as reflected in hypodorsality may cause increased negative mood expressed ventrally, and/or hyperresponsive ventral regions may overwhelm the dorsal regulation system. Research that leverages treatments that differentially improve positive or negative affect/mood may be better able to differentiate the relationships between ventral and dorsal circuits in MDD patients.

Implications for Neurostimulation Therapies

Neuromodulation treatments attempt to influence brain circuits to improve symptoms; however, the focality with which brain regions are targeted differs across modalities. ECT uses specific lead placements (usually right unilateral or bifrontal for depression) to elicit generalized seizures and has been shown to associate with lasting changes throughout the brain, including the hippocampus, thalamus, PFC, dorsal ACC, and other regions (Perrin et al. 2012; Abbott et al. 2013; Tendolkar et al. 2013; Zhang et al. 2013; Dukart et al. 2014; Lyden et al. 2014; van Waarde et al. 2014; Joshi et al. 2015). In the current study, we targeted brain regions with strong differences in RSFC between patients and healthy volunteers prior to analyzing longitudinal effects to reveal novel findings that indicate restored striato-frontal connectivity with ECT. Notably, the ventral striatum and adjacent ventral internal capsule are potential targets of DBS, a more focal and invasive neurostimulation therapy for depression. Two PET studies have demonstrated reductions in medial PFC metabolism subsequent to VS-targeted DBS, including dorsomedial PFC and ventromedial PFC/ACC (Schlaepfer et al. 2008; Bewernick et al. 2010). Thus, VS-targeted DBS also seems to influence functional connections between VS and mediofrontal regions, though ECT and DBS clearly involve different modes of neurostimulation and central nervous system access. In contrast to ECT, however, VS-targeted DBS may be less universally effective in improving symptoms of depression as demonstrated in a recent randomized trial (Dougherty et al. 2015). Future neuroimaging research comparing how the same brain networks (e.g., fronto-striatal) are affected by different neurostimulation therapies may help define the functional circuitry most optimal for stimulation targeting, which could be an important means of improving therapies (Fox et al. 2014).

Conclusions and Additional Considerations

This study presents novel differences in RSFC in patients with severe, unipolar MDD, which support a model of ventral/dorsal imbalance in MDD pathophysiology where the VS and associated striato-thalamo-cortical circuits play an important role. Furthermore, we demonstrate that these MDD-related effects are normalized with ECT, a highly effective therapy for treatment-resistant depression, particularly in regards to hyperconnectivity between VS and a DMN containing ventromedial cortical and limbic structures. These effects may also help elucidate the mechanisms behind other neurostimulation treatments like VS-targeted DBS to improve these therapies. Though our study focused on severe unipolar MDD to lend power to our between-groups effects, future studies that address the heterogeneity of depressive symptoms as they relate to ventral/dorsal imbalance in MDD, bipolar, and other mental disorders may be informative regarding neurobiological links to specific symptom and cognitive dimensions (Insel et al. 2010). Indeed, the relative homogeneity of the current sample may have prevented detection of correlations between cross-sectional effects and depressive symptoms.

Furthermore, future study is warranted to replicate the current results with different cohorts and methodological approaches including exploration of other brain regions of potential relevance to depression (e.g., lateral PFC, lateral parietal cortex, and cerebellum). Here, large multisite studies may better address these and other issues (e.g., sample size, attrition, age of illness onset, ECT lead placement, etc.) that may affect the generalizability of the current results.

Funding

Notes

Conflict of Interest: None declared.

References

Abbott CC, Lemke NT, Gopal S, Thoma RJ, Bustillo J, Calhoun VD, Turner JA. 2013. Electroconvulsive therapy response in major depressive disorder: a pilot functional network connectivity resting state FMRI investigation. Front Psychiatry. 4:10.

Allen EA, Erhardt EB, Damaraju E, Gruner W, Segall JM, Silva RF, Havlicek M, Rachakonda S, Fries J, Kalyanam R, et al. 2011. A baseline for the multivariate comparison of resting-state networks. Front Syst Neurosci. 5:2.

Anand A, Li Y, Wang Y, Lowe MJ, Dzemidzic M. 2009. Resting state corticolimbic connectivity abnormalities in unmedicated bipolar disorder and unipolar depression. Psychiatry Res. 171:189–198.

Anand A, Li Y, Wang Y, Wu J, Gao S, Bukhari L, Mathews VP, Kalnin A, Lowe MJ. 2005. Antidepressant effect on connectivity of the mood-regulating circuit: an FMRI study. Neuropsychopharmacology. 30:1334–1344.

Beckmann CF, Smith SM. 2004. Probabilistic independent component analysis for functional magnetic resonance imaging. IEEE Trans Med Imaging. 23:137–152.

Bewernick BH, Hurlemann R, Matusch A, Kayser S, Grubert C, Hadrysiewicz B, Axmacher N, Lemke M, Cooper-Mahkorn D, Cohen MX, et al. 2010. Nucleus accumbens deep brain stimulation decreases ratings of depression and anxiety in treatment-resistant depression. Biol Psychiatry. 67:110–116.

Bluhm R, Williamson P, Lanius R, Théberge J, Densmore M, Bartha R, Neufeld R, Osuch E. 2009. Resting state default-mode network connectivity in early depression using a seed region-of-interest analysis: decreased connectivity with caudate nucleus. Psychiatry Clin Neurosci. 63:754–761.

Cardinal RN, Parkinson JA, Hall J, Everitt BJ. 2002. Emotion and motivation: the role of the amygdala, ventral striatum, and prefrontal cortex. Neurosci Biobehav Rev. 26:321–352.

Damoiseaux JS, Rombouts SARB, Barkhof F, Scheltens P, Stam CJ, Smith SM, Beckmann CF. 2006. Consistent resting-state networks across healthy subjects. Proc Natl Acad Sci USA. 103:13848–13853.

d'Elia G. 1970. Unilateral electroconvulsive therapy. Acta Psychiatr Scand Suppl. 215:1–98.

De Raedt R, Vanderhasselt M-A, Baeken C. 2014. Neurostimulation as an intervention for treatment resistant depression: from research on mechanisms towards targeted neurocognitive strategies. Clin Psychol Rev. doi:10.1016/j.cpr.2014.10.006.

Di Martino A, Scheres A, Margulies DS, Kelly AM, Uddin LQ, Shehzad Z, Biswal B, Walters JR, Castellanos FX, Milham MP. 2008. Functional connectivity of human striatum: a resting state FMRI study. Cereb Cortex. 18:2735–2747.

Dougherty DD, Rezai AR, Carpenter LL, Howland RH, Bhati MT, O'Reardon JP, Eskandar EN, Baltuch GH, Machado AD, Kondziolka D, et al. 2015. A randomized Sham-controlled trial of deep brain stimulation of the ventral capsule/ventral striatum for chronic treatment-resistant depression. Biol Psychiatry. 78:240–248.

Drevets WC. 2000. Functional anatomical abnormalities in limbic and prefrontal cortical structures in major depression. Prog Brain Res. 126:413–431.

Drevets WC, Price JL, Simpson JR Jr, Todd RD, Reich T, Vannier M, Raichle ME. 1997. Subgenual prefrontal cortex abnormalities in mood disorders. Nature. 386:824–827.

Dukart J, Regen F, Kherif F, Colla M, Bajbouj M, Heuser I, Frackowiak RS, Draganski B. 2014. Electroconvulsive therapy-induced brain plasticity determines therapeutic outcome in mood disorders. Proc Natl Acad Sci USA. 111:1156–1161.

Epstein J, Pan H, Kocsis JH, Yang Y, Butler T, Chusid J, Hochberg H, Murrough J, Strohmayer E, Stern E, et al. 2006. Lack of ventral striatal response to positive stimuli in depressed versus normal subjects. Am J Psychiatry. 163:1784–1790.

Ferry AT, Ongur D, An X, Price JL. 2000. Prefrontal cortical projections to the striatum in macaque monkeys: evidence for an organization related to prefrontal networks. J Comp Neurol. 425:447–470.

Filippini N, MacIntosh BJ, Hough MG, Goodwin GM, Frisoni GB, Smith SM, Matthews PM, Beckmann CF, Mackay CE. 2009. Distinct patterns of brain activity in young carriers of the APOE-epsilon4 allele. Proc Natl Acad Sci USA. 106:7209–7214.

Fox MD, Buckner RL, Liu H, Chakravarty MM, Lozano AM, Pascual-Leone A. 2014. Resting-state networks link invasive and non-invasive brain stimulation across diverse psychiatric and neurological diseases. Proc Natl Acad Sci USA. 111:E4367–E4375.

Fox MD, Snyder AZ, Vincent JL, Corbetta M, Van Essen DC, Raichle ME. 2005. The human brain is intrinsically organized into dynamic, anticorrelated functional networks. Proc Natl Acad Sci USA. 102:9673–9678.

Fox MD, Zhang D, Snyder AZ, Raichle ME. 2009. The global signal and observed anticorrelated resting state brain networks. J Neurophysiol. 101:3270–3283.

Friston KJ, Williams S, Howard R, Frackowiak RSJ, Turner R. 1996. Movement-related effects in fMRI time-series. Magn Reson Med. 35:346–355.

Furman DJ, Hamilton JP, Gotlib IH. 2011. Frontostriatal functional connectivity in major depressive disorder. Biol Mood Anxiety Disord. 1:11.

Galynker II, Cai J, Ongseng F, Finestone H, Dutta E, Serseni D. 1998. Hypofrontality and negative symptoms in major depressive disorder. J Nucl Med. 39:608–612.

Gotlib IH, Joormann J. 2010. Cognition and depression: current status and future directions. Annu Rev Clin Psychol. 6:285–312.

Greicius MD, Flores BH, Menon V, Glover GH, Solvason HB, Kenna H, Reiss AL, Schatzberg AF. 2007. Resting-state functional connectivity in major depression: abnormally increased contributions from subgenual cingulate cortex and thalamus. Biol Psychiatry. 62:429–437.

Groenewold NA, Opmeer EM, de Jonge P, Aleman A, Costafreda SG. 2013. Emotional valence modulates brain functional abnormalities in depression: evidence from a meta-analysis of fMRI studies. Neurosci Biobehav Rev. 37:152–163.

Hamilton JP, Chen G, Thomason ME, Schwartz ME, Gotlib IH. 2011. Investigating neural primacy in Major Depressive Disorder: multivariate Granger causality analysis of resting-state fMRI time-series data. Mol Psychiatry. 16:763–772.

Hamilton JP, Furman DJ, Chang C, Thomason ME, Dennis E, Gotlib IH. 2011. Default-mode and task-positive network activity in major depressive disorder: implications for adaptive and maladaptive rumination. Biol Psychiatry. 70:327–333.

Hauptman JS, DeSalles AAF, Espinoza R, Sedrak M, Ishida W. 2008. Potential surgical targets for deep brain stimulation in treatment-resistant depression. Neurosurg Focus. 25:E3.

Insel T, Cuthbert B, Garvey M, Heinssen R, Pine DS, Quinn K, Sanislow C, Wang P. 2010. Research domain criteria (RDoC): toward a new classification framework for research on mental disorders. Am J Psychiatry. 167:748–751.

Joshi SH, Espinoza RT, Pirnia T, Shi J, Wang Y, Ayers B, Leaver A, Woods RP, Narr KL. 2015. Structural plasticity of the hippocampus and amygdala induced by electroconvulsive therapy in major depression. Biol Psychiatry. doi: 10.1016/j.biopsych.2015.02.029.

Kable JW, Glimcher PW. 2009. The neurobiology of decision: consensus and controversy. Neuron. 63:733–745.

Koenigs M, Grafman J. 2009. The functional neuroanatomy of depression: distinct roles for ventromedial and dorsolateral prefrontal cortex. Behav Brain Res. 201:239–243.

Laird AR, Fox PM, Eickhoff SB, Turner JA, Ray KL, McKay DR, Glahn DC, Beckmann CF, Smith SM, Fox PT. 2011. Behavioral interpretations of intrinsic connectivity networks. J Cogn Neurosci. 23:4022–4037.

Lyden H, Espinoza RT, Pirnia T, Clark K, Joshi SH, Leaver AM, Woods RP, Narr KL. 2014. Electroconvulsive therapy mediates neuroplasticity of white matter microstructure in major depression. Transl Psychiatry. 4:e380.

Manoliu A, Meng C, Brandl F, Doll A, Tahmasian M, Scherr M, Schwerthöffer D, Zimmer C, Förstl H, Bäuml J, et al. 2013. Insular dysfunction within the salience network is associated with severity of symptoms and aberrant inter-network connectivity in major depressive disorder. Front Hum Neurosci. 7:930.

Mayberg HS. 1997. Limbic-cortical dysregulation: a proposed model of depression. J Neuropsychiatry Clin Neurosci. 9:471–481.

Mayberg HS, Liotti M, Brannan SK, McGinnis S, Mahurin RK, Jerabek PA, Silva JA, Tekell JL, Martin CC, Lancaster JL, et al. 1999. Reciprocal limbic-cortical function and negative mood: converging PET findings in depression and normal sadness. Am J Psychiatry. 156:675–682.

Morcom AM, Fletcher PC. 2007. Does the brain have a baseline? Why we should be resisting a rest. Neuroimage. 37:1073–1082.

Murphy K, Birn RM, Handwerker DA, Jones TB, Bandettini PA. 2009. The impact of global signal regression on resting state correlations: are anti-correlated networks introduced? Neuroimage. 44:893–905.

Murray EA. 2007. The amygdala, reward and emotion. Trends Cogn Sci. 11:489–497.

Ongür D, Price JL. 2000. The organization of networks within the orbital and medial prefrontal cortex of rats, monkeys and humans. Cereb Cortex. 10:206–219.

Perrin JS, Merz S, Bennett DM, Currie J, Steele DJ, Reid IC, Schwarzbauer C. 2012. Electroconvulsive therapy reduces frontal cortical connectivity in severe depressive disorder. Proc Natl Acad Sci USA. 109:5464–5468.

Pizzagalli DA, Holmes AJ, Dillon DG, Goetz EL, Birk JL, Bogdan R, Dougherty DD, Iosifescu DV, Rauch SL, Fava M. 2009. Reduced caudate and nucleus accumbens response to rewards in unmedicated individuals with major depressive disorder. Am J Psychiatry. 166:702–710.

Price JL, Drevets WC. 2012. Neural circuits underlying the pathophysiology of mood disorders. Trends Cogn Sci. 16:61–71.

Raichle ME, MacLeod AM, Snyder AZ, Powers WJ, Gusnard DA, Shulman GL. 2001. A default mode of brain function. Proc Natl Acad Sci USA. 98:676–682.

Ray JP, Price JL. 1993. The organization of projections from the mediodorsal nucleus of the thalamus to orbital and medial prefrontal cortex in macaque monkeys. J Comp Neurol. 337:1–31.

Ressler KJ, Mayberg HS. 2007. Targeting abnormal neural circuits in mood and anxiety disorders: from the laboratory to the clinic. Nat Neurosci. 10:1116–1124.

Reynolds SM, Berridge KC. 2002. Positive and negative motivation in nucleus accumbens shell: bivalent rostrocaudal gradients for GABA-elicited eating, taste "Liking"/"Disliking" reactions, place preference/avoidance, and fear. J Neurosci. 22:7308–7320.

Robinson OJ, Cools R, Carlisi CO, Sahakian BJ, Drevets WC. 2012. Ventral striatum response during reward and punishment reversal learning in unmedicated major depressive disorder. Am J Psychiatry. 169:152–159.

Satterthwaite TD, Elliott MA, Gerraty RT, Ruparel K, Loughead J, Calkins ME, Eickhoff SB, Hakonarson H, Gur RC, Gur RE, et al. 2013. An improved framework for confound regression and filtering for control of motion artifact in the preprocessing of resting-state functional connectivity data. Neuroimage. 64:240–256.

Schlaepfer TE, Cohen MX, Frick C, Kosel M, Brodesser D, Axmacher N, Joe AY, Kreft M, Lenartz D, Sturm V. 2008. Deep brain stimulation to reward circuitry alleviates anhedonia in refractory major depression. Neuropsychopharmacology. 33:368–377.

Seymour B, Daw N, Dayan P, Singer T, Dolan R. 2007. Differential encoding of losses and gains in the human striatum. J Neurosci. 27:4826–4831.

Sheehan DV, Lecrubier Y, Sheehan KH, Amorim P, Janavs J, Weiller E, Hergueta T, Baker R, Dunbar GC. 1998. The Mini-International Neuropsychiatric Interview (M.I.N.I.): the development and validation of a structured diagnostic psychiatric interview for DSM-IV and ICD-10. J Clin Psychiatry. 59(Suppl. 2):22–33; quiz 34–57.

Sheline YI, Barch DM, Donnelly JM, Ollinger JM, Snyder AZ, Mintun MA. 2001. Increased amygdala response to masked emotional faces in depressed subjects resolves with antidepressant treatment: an fMRI study. Biol Psychiatry. 50:651–658.

Sheline YI, Barch DM, Price JL, Rundle MM, Vaishnavi SN, Snyder AZ, Mintun MA, Wang S, Coalson RS, Raichle ME. 2009. The default mode network and self-referential processes in depression. Proc Natl Acad Sci USA. 106:1942–1947.

Sheline YI, Sanghavi M, Mintun MA, Gado MH. 1999. Depression duration but not age predicts hippocampal volume loss in medically healthy women with recurrent major depression. J Neurosci. 19:5034–5043.

Siegle GJ, Thompson W, Carter CS, Steinhauer SR, Thase ME. 2007. Increased amygdala and decreased dorsolateral prefrontal BOLD responses in unipolar depression: related and independent features. Biol Psychiatry. 61:198–209.

Smith SM, Fox PT, Miller KL, Glahn DC, Fox PM, Mackay CE, Filippini N, Watkins KE, Toro R, Laird AR, et al. 2009. Correspondence of the brain's functional architecture during activation and rest. Proc Natl Acad Sci USA. 106:13040–13045.

Spreng RN, Grady CL. 2010. Patterns of brain activity supporting autobiographical memory, prospection, and theory of mind, and their relationship to the default mode network. J Cogn Neurosci. 22:1112–1123.

Tendolkar I, van Beek M, van Oostrom I, Mulder M, Janzing J, Voshaar RO, van Eijndhoven P. 2013. Electroconvulsive therapy increases hippocampal and amygdala volume in therapy refractory depression: a longitudinal pilot study. Psychiatry Res. 214:197–203.

Uddin LQ, Kelly AM, Biswal BB, Castellanos FX, Milham MP, Xavier Castellanos F. 2009. Functional connectivity of default mode network components: correlation, anticorrelation, and causality. Hum Brain Mapp. 30:625–637.

van Waarde JA, Scholte HS, van Oudheusden LJB, Verwey B, Denys D, van Wingen GA. 2015. A functional MRI marker may predict the outcome of electroconvulsive therapy in severe and treatment-resistant depression. Mol Psychiatry. 20:609–614.

Victor TA, Furey ML, Fromm SJ, Ohman A, Drevets WC. 2010. Relationship between amygdala responses to masked faces and mood state and treatment in major depressive disorder. Arch Gen Psychiatry. 67:1128–1138.

Winecoff A, Clithero JA, Carter RM, Bergman SR, Wang L, Huettel SA. 2013. Ventromedial prefrontal cortex encodes emotional value. J Neurosci. 33:11032–11039.

Zhang J, Narr KL, Woods RP, Phillips OR, Alger JR, Espinoza RT. 2013. Glutamate normalization with ECT treatment response in major depression. Mol Psychiatry. 18:268–270.

Zimmerman M, Martinez J, Attiullah N, Friedman M, Toba C, Boerescu DA, Rahgeb M. 2012. Further evidence that the cutoff to define remission on the 17-item Hamilton Depression Rating Scale should be lowered. Depress Anxiety. 29:159–165.